MHD boundary layer flow of Casson fluid passing through an exponentially stretching permeable surface with thermal radiation

Swati Mukhopadhyay[a)†], Iswar Chandra Moindal[a)‡], and Tasawar Hayat[b)c)§]

[a)] *Department of Mathematics, The University of Burdwan, Burdwan-713104, W. B., India*
[b)] *Department of Mathematics, Quaid-i-Azam University 45320, Islamabad, Pakistan*
[c)] *Department of Mathematics, Faculty of Science, King Abdulziz University, Jeddah 21589, Saudi Arabia*

(Received 23 October 2013; revised manuscript received 25 March 2014; published online 10 August 2014)

This article numerically examines the boundary layer flow due to an exponentially stretching surface in the presence of an applied magnetic field. Casson fluid model is used to characterize the non-Newtonian fluid behavior. The flow is subjected to suction/blowing at the surface. Analysis is carried out in presence of thermal radiation and prescribed surface heat flux. In this study, an exponential order stretching velocity and prescribed exponential order surface heat flux are accorded with each other. The governing partial differential equations are first converted into nonlinear ordinary differential equations by using appropriate transformations and then solved numerically. The effect of increasing values of the Casson parameter is to suppress the velocity field. However the temperature is enhanced when Casson parameter increases. It is found that the skin-friction coefficient increases with increasing values of suction parameter. Temperature also increases for large values of power index n in both suction and blowing cases at the boundary. It is observed that the thermal radiation enhances the effective thermal diffusivity and hence the temperature rises.

Keywords: exponential stretching, suction/blowing, prescribed heat flux, thermal radiation

PACS: 47.15.Cb, 44.20.+b, 47.50.−d **DOI:** 10.1088/1674-1056/23/10/104701

1. Introduction

Dynamics of non-Newtonian fluid is quite a popular topic of research among the recent investigators. Such interest, in fact, stems from the applications of these fluids in biology, physiology, technology, and industry. Besides this, the flow of non-Newtonian fluids with heat transfer has great importance in engineering applications such as the thermal design of industrial equipment dealing with polymeric liquids, molten plastics, and food stuffs or slurries. Various non-Newtonian models in general have nonlinear relationship between stress and rate of strain. The classification of these models have been presented through three categories known as differential, rate, and integral. Several researchers in the field are making progress by considering subclasses of categories in three different flow configurations.[1–11]

Casson fluid is one of the non-Newtonian fluid models, which exhibits yield stress. If a shear stress less than the yield stress is applied to the fluid then it behaves like a solid and such a fluid moves when shear stress greater than the yield stress is applied. Examples of Casson fluid include jelly, tomato sauce, honey, soup, concentrated fruit juices, etc. Human blood can also be treated as Casson fluid. Due to the presence of several substances like, protein, fibrinogen, and globulin in an aqueous-base plasma, human red blood cells can form a chainlike structure, known as aggregates or rouleaux. If the rouleaux behaves like a plastic solid then there exists a yield stress that can be identified with the constant yield stress in Casson fluid.[11] Casson fluid can be defined as a shear thinning liquid which is assumed to have an infinite viscosity at zero rate of shear, a yield stress below which no flow occurs, and a zero viscosity at an infinite rate of shear.[12] Eldabe and Salwa[13] have studied the Casson fluid for the flow between two rotating cylinders. Boyd *et al.*[14] investigated the Casson fluid flow for the oscillatory blood flow. Nadeem *et al.*[15] investigated the three-dimensional Casson fluid flow over a linearly porous stretching sheet in the presence of an external magnetic field.

The study of laminar flow and heat transfer over a stretching sheet is of considerable interest due to their everincreasing industrial applications and important bearings in several technological processes. Boundary layer flow over a stretching surface is often encountered in many engineering disciplines. Most of the existing literature on this topic deals with the study of boundary layer flow over a linear stretching surface. However, it is often argued that realistically stretching of plastic sheet may not necessarily be linear.[16] Magyari and Keller[17] studied the heat and mass transfer in boundary layer flow induced by an exponentially continuous stretching sheet. Elbashbeshy[18] investigated the flow caused by exponentially continuous stretching surface. Partha *et al.*[19] analyzed the effect of viscous dissipation in the mixed convection

†Corresponding author. E-mail: swati_bumath@yahoo.co.in
‡E-mail: iswar.chandra2010@gmail.com
§E-mail: pensy_t@yahoo.com

© 2014 Chinese Physical Society and IOP Publishing Ltd

flow from an exponentially stretching surface in a quiescent viscous fluid. Khan[20] and Sanjayanand and Khan[21] studied the viscoelastic boundary layer flow and heat transfer by an exponentially stretching sheet. Al-Odat *et al.*[22] discussed the effects of magnetic field on flow and heat transfer passing through an exponentially stretching surface. Later, Sajid and Hayat[23] considered the influence of thermal radiation on the boundary layer flow due to an exponentially stretching sheet. Bidin and Nazar[24] analyzed the effect of thermal radiation on the steady laminar two-dimensional boundary layer flow and heat transfer over an exponentially stretching sheet. Bararnia *et al.*[25] analytically studied the boundary layer flow and heat transfer on continuously stretching surface by taking into account exponential surface velocity and temperature distribution. El-Aziz[26] investigated the mixed convection flow of micropolar fluid passing through an exponentially stretching sheet. Pal[27] reported mixed convection flow passing through an exponentially stretching surface in presence of a magnetic field. Nadeem *et al.*[28] analyzed the flow of Jeffrey fluid and heat transfer by an exponentially stretching sheet. Ishak[29] discussed the combined effects of magnetic field and thermal radiation on flow and heat transfer over an exponentially stretching sheet. Sahoo and Poncet[30] addressed the flow of third grade fluid passing through an exponentially stretching sheet in the presence of partial slip. Mukhopadhyay and Gorla[31] discussed the effects of partial slip on the flow passing through an exponentially stretching sheet. Nadeem *et al.*[32] investigated the effects of magnetic field on Casson fluid flow passing through an exponentially shrinking sheet.

The process of suction or blowing has also its importance in many engineering activities, for example, in the design of thrust bearing and radial diffusers, and thermal oil recovery. Suction or injection (blowing) of a fluid through the bounding surface can significantly change the flow field. Suction is applied to chemical processes to remove reactants whereas blowing is used to add reactants, cool the surface, prevent corrosion or scaling and reduce the drag.

On the other hand, the problems with variable surface heat flux have been introduced in many other studies.[33–36] In modeling the boundary layer flow and heat transfer of these problems, the boundary conditions in the past are usually imposed either on surface temperature or a specified surface heat flux. Liu[37] investigated the hydromagnetic flow over a linearly stretching sheet by considering both prescribed surface temperature and prescribed surface heat flux conditions. Ishak *et al.*[38] discussed the heat transfer characteristics for moving plate in a parallel stream with surface heat flux. Aman and Ishak[39] investigated MHD mixed convection boundary layer flow adjacent to a stretching vertical sheet with prescribed surface heat flux. Recently, Bhattacharyya[40] analyzed the effects of variable heat flux on stagnation-point flow towards a shrinking sheet.

The objective of the present article is to investigate the flow and heat transfer analysis in boundary layer flow of Casson fluid over an exponentially stretching sheet when both magnetic field and thermal radiation are present. To the best of author's knowledge, effects of thermal radiation and variable heat flux on Casson fluid flow passing through an exponentially stretching surface have not yet been addressed in the literature. In this article, combined effects of suction/blowing and prescribed heat flux are also studied. Exponential order surface heat flux is considered. Transformation method is employed in obtaining the third-order differential equation from the momentum equation and the second-order equation by energy law. Numerical calculations up to desired level of accuracy are carried out for different values of dimensionless parameters of the problem under consideration. Comparison is made with the available results from the literature, and an excellent agreement is found. Analysis of the results shows that the flow field is influenced appreciably by the prescribed heat flux in the presence of magnetic field, suction or injection at the wall and thermal radiation. It is expected that the results obtained will not only provide useful information for applications but also serve as a complement to the previous studies.

2. Governing equations

Consider a flow of an incompressible viscous electrically conducting fluid induced by an exponential sheet at $y = 0$. Besides this, the heat transfer analysis with thermal radiation effect is taken into account. The fluid is electrically conducting in the presence of a non-uniform magnetic field $B(x) = B_0 \mathrm{e}^{x/(2L)}$ (which is normal to the sheet, B_0 being a constant). Rheological equation of state for an isotropic and incompressible flow of Casson fluid is given by

$$\tau_{ij} = \begin{cases} 2(\mu_{\mathrm{B}} + p_{\mathrm{y}}/\sqrt{2\pi})e_{ij}, & \pi > \pi_{\mathrm{c}}, \\ 2(\mu_{\mathrm{B}} + p_{\mathrm{y}}/\sqrt{2\pi_{\mathrm{c}}})e_{ij}, & \pi < \pi_{\mathrm{c}}. \end{cases}$$

Here, $\pi = e_{ij}e_{ij}$ and e_{ij} is the (i, j)-th component of the deformation rate, π is the product of the component of deformation rate with itself, π_{c} is a critical value of this product based on the non-Newtonian model, μ_{B} is plastic dynamic viscosity of the non-Newtonian fluid, and p_{y} is the yield stress of the fluid.

The equations in the present flow under consideration are given by

$$\frac{\partial u}{\partial x} + \frac{\partial \upsilon}{\partial y} = 0, \tag{1}$$

$$u\frac{\partial u}{\partial x} + \upsilon\frac{\partial u}{\partial y} = \nu\left(1 + \frac{1}{\beta}\right)\frac{\partial^2 u}{\partial y^2} - \frac{\sigma B^2}{\rho}u, \tag{2}$$

$$u\frac{\partial T}{\partial x} + \upsilon\frac{\partial T}{\partial y} = \kappa\frac{\partial^2 T}{\partial y^2} - \frac{1}{\rho c_p}\frac{\partial q_{\mathrm{r}}}{\partial y}. \tag{3}$$

Here, u and v are the components of velocity respectively in the x and y directions, ν is the kinematic viscosity, ρ is the fluid density (assumed to be constant), $\beta = \mu_B\sqrt{2\pi_c}/p_y$ is the parameter of the Casson fluid, σ is the electrical conductivity, κ is the thermal diffusivity of the fluid, q_r is the radiative heat flux, and c_p is the specific heat at constant pressure. In writing the above equations, the induced magnetic field is neglected due to small magnetic Reynolds number.

Using the Rosseland approximation for radiation (Brewster[41]) we can write

$$q_r = -\frac{4\sigma^*}{3k^*}\frac{\partial T^4}{\partial y},$$

where σ^* is the Stefan–Boltzman constant and k^* is the absorption coefficient. Assuming that the temperature difference within the flow is such that T^4 may be expanded in a Taylor series, expanding T^4 about the free stream temperature T_∞ and neglecting higher orders we obtain $T^4 \equiv 4T_\infty^3 T - 3T_\infty^4$. Therefore, equation (3) becomes

$$u\frac{\partial T}{\partial x} + v\frac{\partial T}{\partial y} = \kappa\frac{\partial^2 T}{\partial y^2} + \frac{16\sigma^* T_\infty^3}{3\rho c_p k^*}\frac{\partial^2 T}{\partial y^2}. \tag{4}$$

2.1. Boundary conditions

The appropriate boundary conditions for the problem are imposed as follows:

$$\text{at } y = 0,\ u = U,\ v = -V(x),\ \frac{\partial T}{\partial y} = -\frac{q_w(x)}{\kappa}, \tag{5a}$$

$$\text{as } y \to \infty,\ u \to 0,\ T \to T_\infty. \tag{5b}$$

Here, $U = U_0 e^{x/L}$ is the stretching velocity;[16] $q_w(x) = q_{w0}T_0\sqrt{U_0/(2\nu L)}e^{nx/L}$ is the variable surface heat flux;[27] U_0, T_0, and q_{w0} are the reference velocity, temperature, and heat flux respectively; $V(x) = V_0 e^{x/(2L)}$, a special type of velocity at the wall is considered[42] where V_0 is a constant. Here $V(x) > 0$ is the velocity of suction and $V(x) < 0$ is the velocity of blowing.

2.2. Method of solution

Introducing the variables as follows:

$$\eta = \sqrt{\frac{U_0}{2\nu L}}e^{x/(2L)}y, \tag{6a}$$

$$u = U_0 e^{x/L}f'(\eta), \tag{6b}$$

$$v = -\sqrt{\nu U_0/(2L)}e^{x/(2L)}\{f(\eta) + \eta f'(\eta)\}, \tag{6c}$$

$$T = T_\infty + \frac{q_{w0}}{\kappa}T_0 e^{nx/(2L)}\theta(\eta), \tag{6d}$$

and substituting Eqs. (6) into Eqs. (2) and (4), the governing equations are reduced to the following equations:

$$\left(1+\frac{1}{\beta}\right)f''' + ff'' - 2f'^2 - M^2 f' = 0, \tag{7}$$

$$\left(1+\frac{4}{3}R\right)\theta'' + Pr(f\theta' - nf'\theta) = 0, \tag{8}$$

and the boundary conditions are

$$\text{at } \eta = 0,\ f' = 1,\ f = S,\ \theta' = -1, \tag{9}$$

$$\text{and as } \eta \to \infty,\ f' \to 0,\ \theta \to 0, \tag{10}$$

where the prime denotes differentiation with respect to similarity variable η, $S = V_0/\sqrt{U_0\nu/(2L)} > 0$ (or < 0) is the suction (or blowing) parameter, $M = \sqrt{2\sigma B_0^2 L/(\rho U_0)}$ is the magnetic parameter, $R = 4\sigma^* T_\infty^3/(k^*\kappa)$ is the radiation parameter, and $Pr = \nu/\kappa$ is the Prandtl number, κ is the coefficient of thermal diffusivity, ρ is the density of fluid, ν is the kinematic viscosity, and θ is the non-dimensional temperature. We further note that equation (1) is clearly satisfied.

3. Numerical method

Equations (7) and (8) subject to the boundary conditions (9) and (10) are solved by converting these to an initial value problem. We set

$$f' = z,\ z' = p,\ \theta' = q,$$

$$p' = (2z^2 - fp + M^2 z)\Big/\left(1+\frac{1}{\beta}\right), \tag{11}$$

$$q' = Pr(nz\theta - fq)\Big/\left(1+\frac{4}{3}R\right) \tag{12}$$

with the boundary conditions

$$f(0) = S,\ f'(0) = 1,\ \theta'(0) = -1. \tag{13}$$

In order to integrate Eqs. (11) and (12) into an initial value problem we require a value for $p(0)$, i.e., $f''(0)$ and $\theta(0)$ but no such values are given on the boundary. The most important factor of shooting method is to choose the appropriate finite value of η_∞. In order to determine η_∞ for the boundary value problem stated by Eqs. (11)–(13), we start with some initial guess for some particular set of physical parameters in order to obtain $f''(0)$ and $\theta(0)$. The solution procedure is repeated with another large value of η_∞ until two successive values of $f''(0)$ and $\theta(0)$ differ only by the specified significant digit. The last value of η_∞ is finally chosen to be the most appropriate value of the limit η_∞ for that particular set of parameters. The value of η_∞ may change for another set of physical parameters. Once the finite value of η_∞ is determined, the integration is carried out. We compare the calculated values for f' and θ at $\eta = 10$ (say) with the given boundary conditions $f'(10) = 0$ and $\theta(10) = 0$ and adjust the estimated values, $f''(0)$ and $\theta(0)$, to obtain a better approximation for the solution.

We take a series of values for $f''(0)$ and $\theta(0)$, and use the fourth-order classical Runge–Kutta method with step-size $h = 0.01$. The above procedure is repeated until we obtain the results up to the desired degree of accuracy 10^{-5}.

4. Results and discussion

4.1. Validation of results

To judge the correct running of the program the value of the missing initial condition $f''(0)$ for Newtonian fluid is compared with the values reported by Magyari and Keller,[17] Elbashbeshy,[18] Sahoo and Poncet[30] in their pioneering studies and found to be in good agreement with their results (see Table 1).

For the verification of accuracy of the applied numerical scheme, a comparison of the results obtained for prescribed surface temperature instead of variable surface heat flux is made. For this calculation we consider the boundary conditions for temperature as follows:

$$\text{at } y=0,\ T=T_{\rm w} \text{ and as } y\to\infty,\ T\to T_{\infty},$$

where $T_{\rm w}=T_{\infty}+T_0\,{\rm e}^{nx/(2L)}$ is the temperature at the sheet.

These conditions finally take the following forms:

$$\text{at } \eta=0,\ \theta=1 \text{ and as } \eta\to\infty,\ \theta\to 0. \qquad \text{(PST)}$$

Comparison is made of the results corresponding, for prescribed surface temperature (PST), to the values of heat transfer coefficient $[-\theta'(0)]$ for Newtonian fluid and $S=0$ (i.e., in the absence of suction/blowing at the boundary) and for $n=1$ with the available published results of Magyari and Keller,[17] Bidin and Nazar,[24] El-Aziz,[26] and Ishak[29] (for some special cases) (see Table 2). The results are found to be in excellent agreement. Moreover, the results corresponding to the values of heat transfer coefficient $[-\theta'(0)]$ for Newtonian fluid and $S=0$ (i.e. in the absence of suction/blowing at the boundary) are compared with those of Magyari and Keller,[17] Al-Odat *et al.*,[22] and Pal[27] (for some special cases) for variable values of power index n of surface temperature and for variable Prandtl number (see Table 3). The results are found to agree well with those of Magyari and Keller[17] and Pal[27] but differ slightly from those of Al-Odat *et al.*[22]

Table 1. Values of $f''(0)$ for Newtonian fluid in the absence of magnetic field and in the case of non-permeable stretching sheet.

Magyari Keller[17]	Elbashbeshy[18]	Sahoo and Poncet[30]	Present study
−1.28180	−1.28181	−1.281811	−1.281812

Table 2. Values of $[-\theta'(0)]$ (PST case) for several values of Prandtl number in Newtonian fluid.

Pr	R	M	Magyari and Keller[17]	Bidin and Nazar[24]	El-Aziz[26]	Ishak[29]	Present study with $S=0$, $n=1$
1	0	0	0.9548	0.9547	0.9548	0.9548	0.9547
2				1.4714		1.4715	1.4714
3			1.8691	1.8691	1.8691	1.8691	1.8691
5			2.5001		2.5001	2.5001	2.5001
10			3.6604		3.6604	3.6604	3.6603
1		1				0.8611	0.8610
	1	0		0.5315		0.5312	0.5311
		1				0.4505	0.4503

Table 3. Values of $[\theta'(0)]$ (PST case) for several values of Prandtl number and power index n in Newtonian fluid.

n	Magyari and Keller[17]		Al-Odat *et al.*[22] $H_{\rm a}=0=E_{\rm c}=\lambda$		Pal[27] with $H_{\rm a}=0=G_{\rm r}=E_{\rm c}=\lambda$		Present study $S=0=M=R$	
	$Pr=0.5$	$Pr=1$	$Pr=0.5$	$Pr=1$	$Pr=0.5$	$Pr=1$	$Pr=0.5$	$Pr=1$
−0.5	−0.17582	−0.29988	−0.18187	−0.32697	−0.17582	−0.29988	−0.17582	−0.29988
0	−0.33049	−0.54964	−0.31006	−0.53104	−0.33049	−0.54964	−0.33049	−0.54964
1	−0.59434	0 − 0.95478	−0.57771	−0.91903	−0.59434	−0.95478	−0.59434	−0.95478

4.2. Effects of different physical parameters on flow and temperature fields

In order to analyze the results, numerical computations are carried out by using the method described in the previous section for various values of Casson fluid parameter (β), suction/blowing parameter (S), power index (n), and Prandtl number (Pr). For illustrations of the results, the numerical values are plotted in Figs. 1–7.

We first concentrate on the effects of Casson parameter β on velocity and temperature profiles. Figure 1(a) depicts the effects of Casson fluid parameter β on the velocity profiles for permeable sheet (i.e., in the presence of suction/blowing) in presence of magnetic field. Velocity is found to decrease with increasing the value of Casson parameter β. Due to increase in β, plastic dynamic viscosity increases and it causes resistance to fluid motion. Reducing nature of the momentum boundary layer thickness is noted when β increases and hence induces an increase in the absolute value of the velocity gradient at the surface. Fluid velocity is much more suppressed in the case of suction ($S=0.5$) than that of blowing ($S=-0.5$) [Fig. 1(a)].

The nature of temperature profiles for variable values of Casson fluid parameter β over permeable stretching sheet (i.e., in the presence of suction/blowing) and also for the positive and negative values of power index n are presented in

Figs. 1(b) and 1(c) respectively. Temperature at a point increases in this case. Thermal boundary layer thickness increases with increasing β. The thickening of the thermal boundary layer occurs due to the increase in elasticity stress parameter. At a fixed point, temperature is higher for negative value of power index n than that for positive value of power index n [Figs. 1(b) and 1(c)]. Both figures clearly show that with increasing Casson fluid parameter β, the temperature is found to increase for both cases of suction and blowing [Figs. 1(b) and 1(c)]. On the other hand, an increase in temperature field is much more pronounced in the case of blowing ($S=-0.5$) than in the case of suction ($S=0.5$) [Figs. 1(b) and 1(c)]. For negative value of power index n, the temperature is higher than that for positive value of power index n.

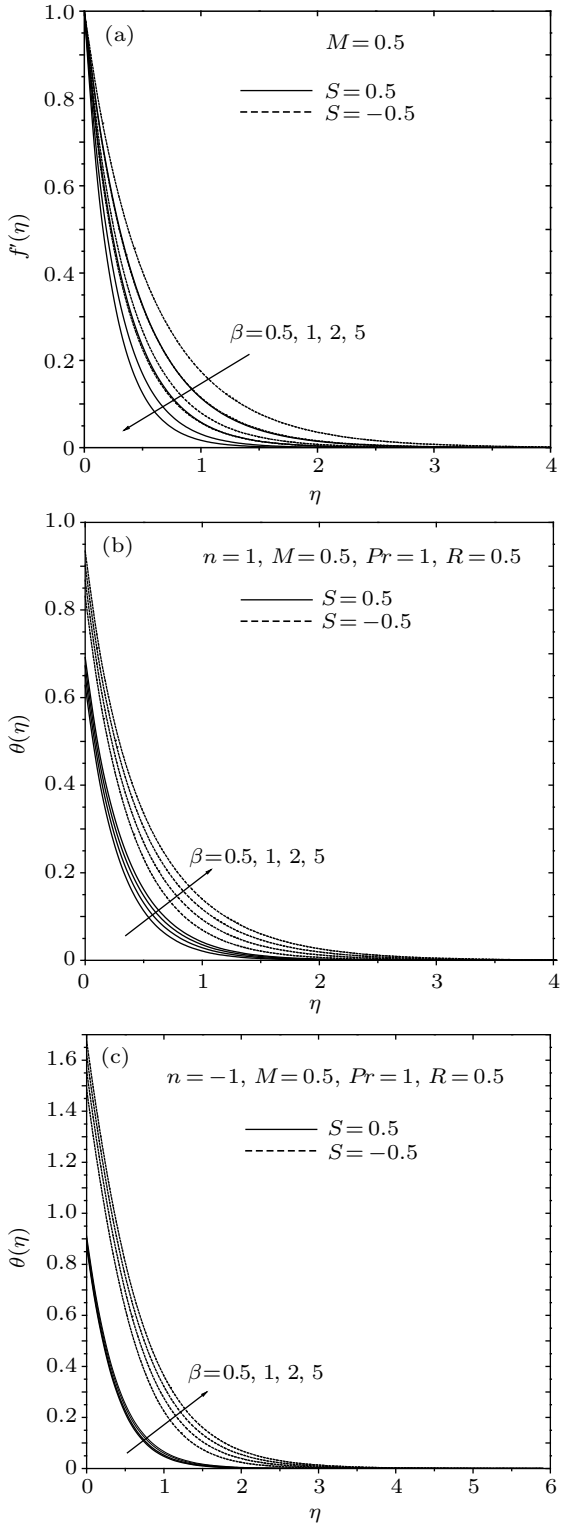


Fig. 1. Variations of velocity $f'(\eta)$ with η for several values of Casson fluid parameter β in the presence of suction/blowing (a); variations of temperature $\theta(\eta)$ with η for several values of Casson fluid parameter β in the presence of suction/blowing for positive (b), and negative (c) values of power index n of surface heat flux.

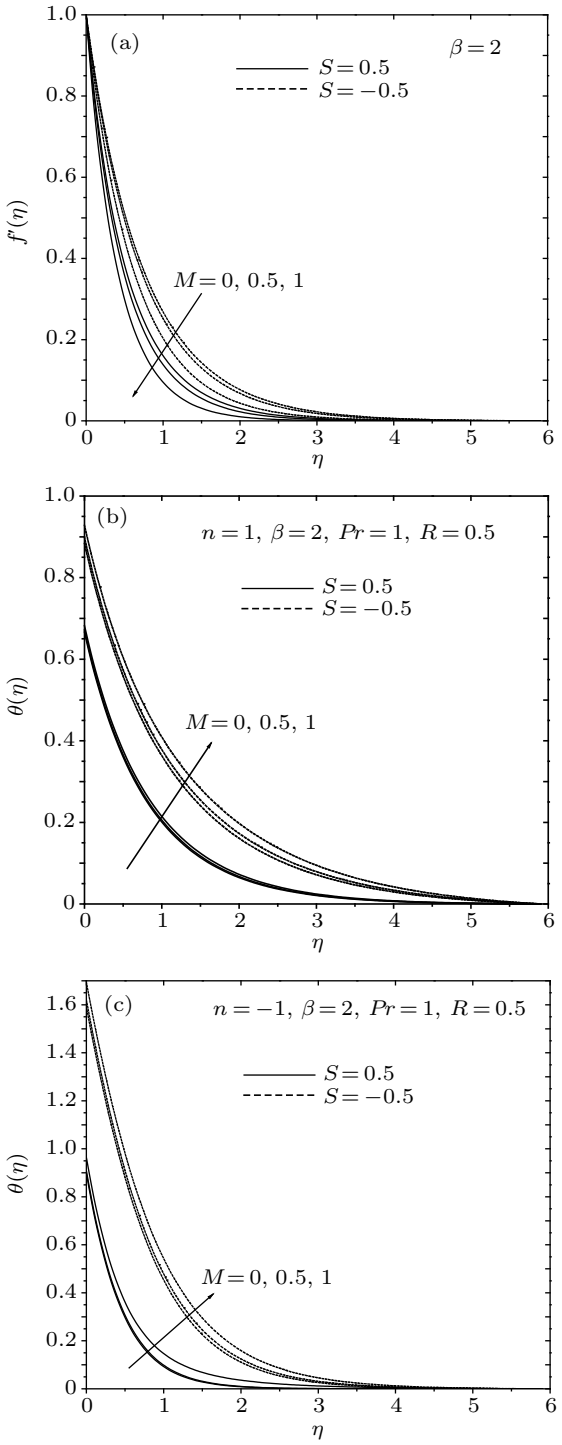


Fig. 2. Variations of velocity $f'(\eta)$ with η for several values of magnetic parameter M in the presence of suction/blowing (a); variations of temperature $\theta(\eta)$ with η for several values of M in the presence of suction/blowing for positive (b), and negative (c) values of power index n of surface heat flux.

Effects of magnetic field on velocity and temperature field in the presence of suction/blowing are exhibited in Figs. 2(a)–2(c). With increasing the value of magnetic parameter, the fluid velocity decreases [Fig. 2(a)] whereas the temperature is found to increase both in the case for the positive value of power index n [Fig. 2(b)] and in the case of negative value of power index n [Fig. 2(c)]. The transverse magnetic field induces drag in terms of Lorentz force which opposes the motion of the fluid and the rate of transport is considerably reduced. This is because with the increase in M, Lorentz force increases and it produces more resistance to the flow. As M increases, the thermal boundary layer thickness increases [Figs. 2(b) and 2(c)]. The temperature is higher when n is negative.

Figure 3(a) exhibits the effects of suction/blowing parameter S on velocity profile for exponentially stretching sheet. It is observed that in the presence of the magnetic field, velocity decreases significantly with increasing suction whereas the fluid velocity is found to increase with augment of blowing [Fig. 3(a)]. It is observed that there is a decrease in boundary layer thickness and the velocity field is also reduced when $S > 0$. Opposite behavior is seen for blowing ($S < 0$) when compared with suction. The physical reason for such a behavior is that while stronger blowing is provided, the heated fluid is pushed farther from the wall where the flow is accelerated due to less influence of the viscosity. This effect leads to the increase of maximum velocity within the boundary layer. The same principle operates but in a reverse direction in the case of suction. Figure 3(b) shows the temperature profiles for variable suction/blowing parameter S and also for positive value of power index n. It is seen that temperature decreases with increasing suction whereas it increases in blowing [Fig. 3(b)]. Temperature at a point is higher for negative value of power index n than that for positive value of power index n [Fig. 3(b)]. Temperature field becomes much more suppressed in suction case. Actually, the effect of suction is to make the velocity and temperature distribution more uniform within the boundary layer. Imposition of fluid suction at the surface has a tendency to reduce both the hydrodynamic and thermal thickness of the boundary layer where viscous effect is dominant. This leads to reduction of both the fluid velocity and temperature. Also the thermal boundary layer thickness increases with the increase of injection which causes the rate of heat transfer to decrease.

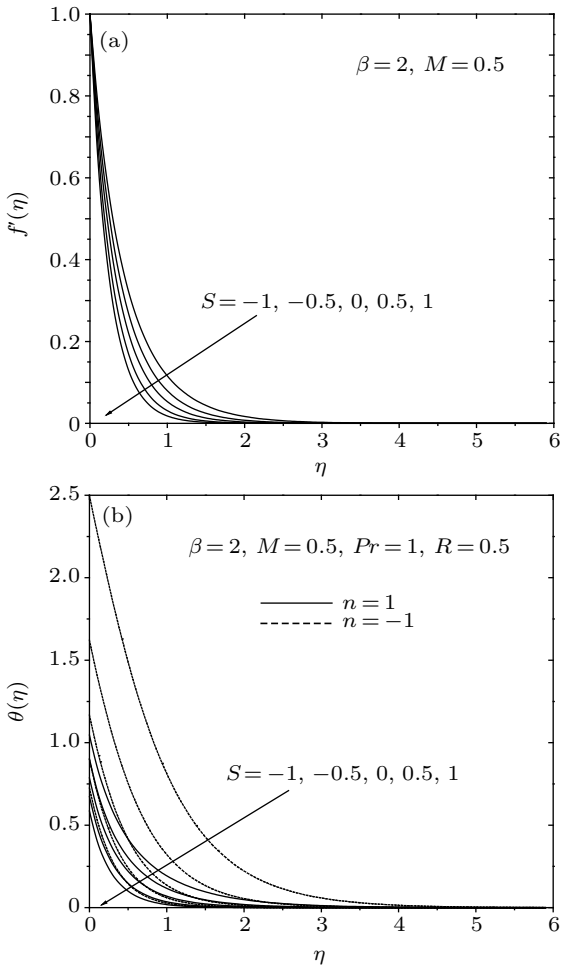


Fig. 3. Variations of velocity $f'(\eta)$ with η for several values of suction/blowing parameter S (a); variations of temperature $\theta(\eta)$ with η for several values of suction/blowing parameter S for positive/negative values of power index n of surface heat flux (b).

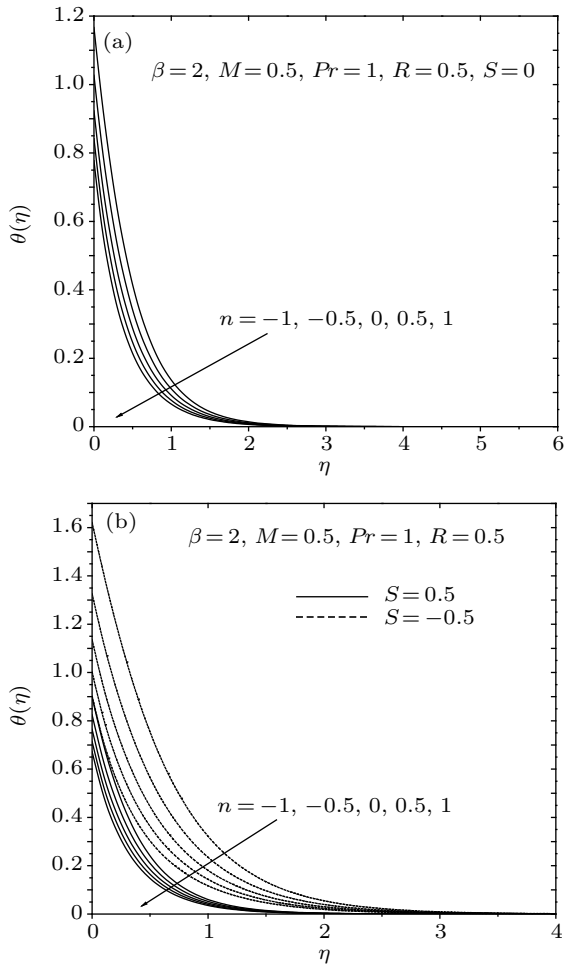


Fig. 4. Variations of temperature $\theta(\eta)$ with η for several values of power index n of surface heat flux in the absence (a) and the presence (b) of suction/blowing.

Figures 4(a) and 4(b) display the temperature fields for

variable values of power index n respectively in the absence and in the presence of suction $(S = 0.5)$/blowing $(S = -0.5)$. In both cases the temperature decreases with increasing the value of power index n due to reducing nature of the thermal boundary layer thickness with increasing n. It is interesting to note from this figure that the wall temperature decreases throughout in the boundary layer for positive values of n (i.e., the heat transfer is directed from the wall to the ambient fluid).

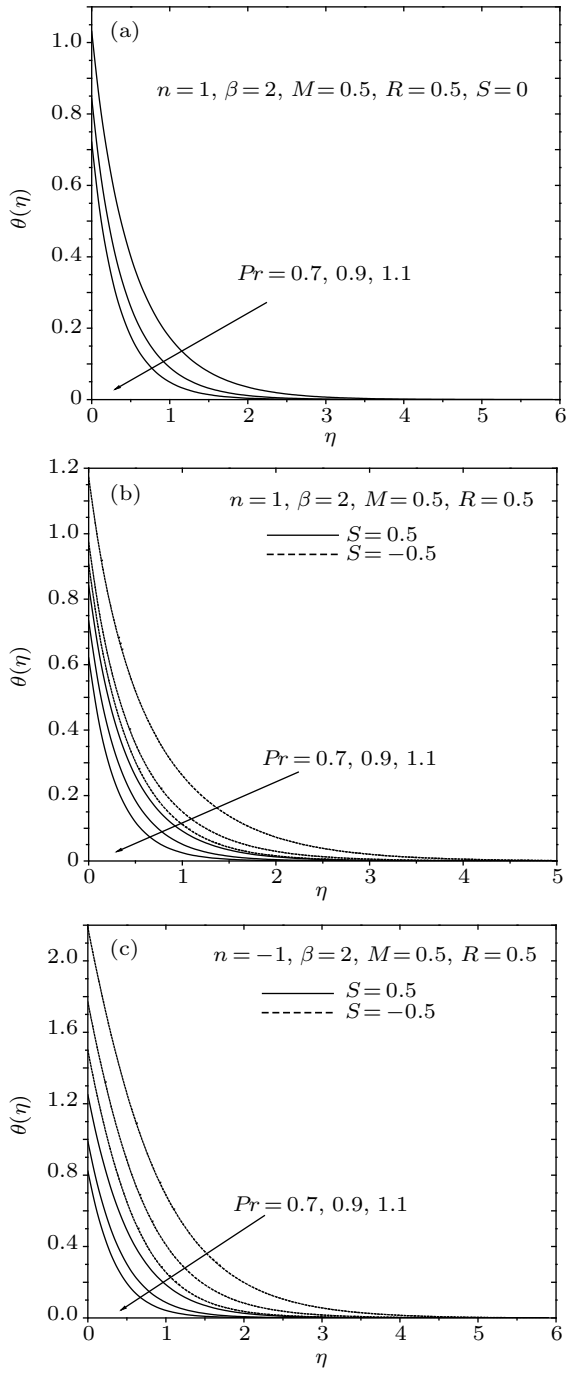


Fig. 5. Variations of temperature $\theta(\eta)$ with η for several values of Prandtl number Pr in the absence of suction and positive value of power index n of surface heat flux (a); variations of temperature $\theta(\eta)$ with η for several values of Prandtl number Pr in the presence of suction/blowing and positive (b), and negative (c) values of power index n of surface heat flux.

Figure 5(a) depicts the effects of Prandtl number Pr on temperature profile in the absence $(S = 0)$ of suction/blowing at the boundary for positive power index n. The temperature decreases with increasing Pr. An increase in Prandtl number reduces the thermal boundary layer thickness. Prandtl number signifies the ratio of momentum diffusivity to thermal diffusivity. In heat transfer problems, the Prandtl number Pr controls the relative thickening of the momentum and thermal boundary layers. When Prandtl number Pr is small, heat diffuses quickly compared with the velocity (momentum), which means that for liquid metals, the thickness of the thermal boundary layer is much larger than the momentum boundary layer. Fluids with lower Prandtl number have higher thermal conductivities (and thicker thermal boundary layer structures) so that heat can diffuse from the sheet faster than higher Pr fluids (thinner boundary layers). Hence Prandtl number can be used to increase the cooling rate in a flow. For positive power index n, figure 5(b) shows the nature of temperature profiles for variable values of Prandtl number in the presence of suction/blowing $(S = 0.5,\ -0.5)$. Moreover, the thermal boundary layer thickness decreases with increasing Prandtl number [Fig. 5(b)]. It is also noted that wall-temperature gradient is

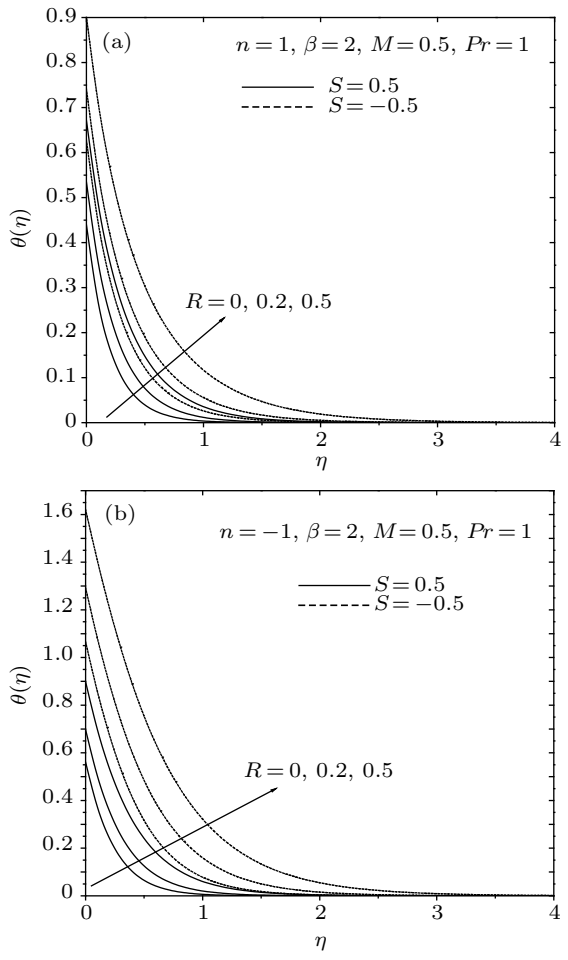


Fig. 6. Variations of temperature $\theta(\eta)$ with η for several values of radiation parameter R in presence of suction/blowing and positive (a) and negative (b) values of power index n of surface heat flux.

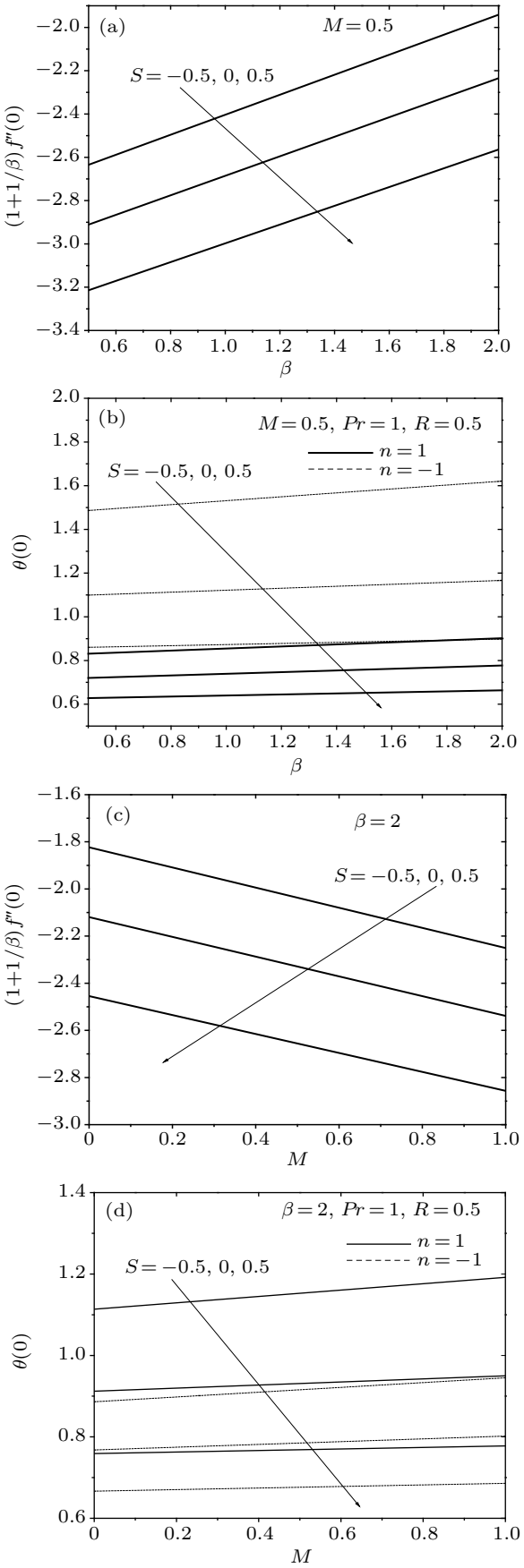


Fig. 7. Skin-friction coefficient via Casson fluid parameter β (a) and magnetic parameter M (c) for variable values of suction/injection parameter S; wall temperature $\theta(0)$ via Casson fluid parameter β (b) and magnetic parameter M (d), for two values of power index n of surface heat flux and also for three values of suction/injection parameter S.

positive for all values of the Prandtl number. Physically it means that the heat is always transferred from the ambient fluid to the surface. The wall-temperature gradient $\theta'(0)$ increases with increasing Pr. Temperature profiles for variable values of Pr in the presence of suction/blowing for $n = -1$ are shown in Fig. 5(c). Here also, the temperature decreases with increasing values of Prandtl number Pr.

Figures 6(a) and 6(b) display the nature of temperature fields for variable values of radiation parameter R respectively for positive and negative values of power index n. In both cases temperature is found to increase with increasing R. Thermal boundary layer thickness increases as R increases.

Figure 7(a) exhibits the nature of skin-friction coefficient with Casson fluid parameter β for three values of suction/blowing parameter S. It is found that skin-friction coefficient increases with increasing β and it is higher for suction than that for blowing. From this figure it is very clear that shear stress at the wall is negative. Physically, negative sign of $f''(0)$ implies that surface exerts a dragging force on the fluid and positive sign implies the contrary scenario. Figure 7(b) displays the nature of wall temperature $[\theta(0)]$ against the Casson fluid parameter β for both positive and negative values of power index n. Wall temperature increases with increasing β. The local Nusselt number $1/\theta(0)$ is always positive, which means that the heat is transferred from the hot sheet to the cool fluid. An increase of Casson fluid parameter β leads to an increase in the heat transfer coefficient. Wall temperature $\theta(0)$ increases with blowing but decreases with suction [Fig. 7(b)]. Heat transfer coefficient increases with increasing the value of power index n [Fig. 7(b)]. Skin friction coefficient increases with increasing the value of magnetic parameter M [Fig. 7(c)]. So, magnetic parameter M can be used as a controlling parameter to control the surface shear stress. Wall temperature $\theta(0)$ increases with the increase in M [Fig. 7(d)].

5. Conclusions

The present study provides the numerical solutions for steady boundary layer flow and heat transfer in a Casson fluid over an exponentially permeable stretching surface with prescribed heat flux. The main findings of this investigation can be summarized as follows.

(i) Momentum boundary layer thickness decreases with increasing Casson fluid parameter but the thermal boundary layer thickness increases in this case.

(ii) Effect of suction parameter on viscous incompressible fluid is to suppress the velocity field which in turn causes the enhancement of the skin-friction coefficient.

(iii) Skin-friction coefficient is higher for suction than for blowing.

(iv) The surface shear stress increases as the magnetic and Casson fluid parameters increase.

(v) Magnetic parameter reduces the rate of transport.

(vi) Temperature decreases with increasing the value of power index n.

(vii) Thermal boundary layer thickness decreases with increasing the value of power index n.

(viii) Thermal boundary layer thickness increases with the increase in magnetic parameter and radiation parameter.

(ix) Wall temperature increases with increasing the magnetic parameter.

(x) Temperature decreases with increasing Prandtl number Pr and an increase in Prandtl number reduces the thermal boundary layer thickness.

References

[1] Tan W C and Masuoka T 2005 *Phys. Fluids* **17** 023101
[2] Pakdemirli M 1992 *Int. J. Non-Linear Mech.* **27** 785
[3] Yang D and Zhu K Q 2010 *Comput. Math. Appl.* **60** 2231
[4] Zierep J and Fetecau C 2007 *Int. J. Eng. Sci.* **45** 155
[5] Serdar B and Salih Dokuz 2006 *Int. J. Eng. Sci.* **44** 49
[6] Hayat T, Zaib S, Asghar S and Hendi A A 2012 *Appl. Math. Mech.* **33** 411
[7] Aksoy Y, Pakdemirli M and Khalique C M 2007 *Int. J. Eng. Sci.* **45** 829
[8] Zhao C and Yang C 2011 *J. Non-Newtonian Fluid Mech.* **166** 1076
[9] Ellahi R, Hayat T and Asghar S 2010 *Nonlinear Anal.: Real World Appl.* **11** 139
[10] Hayat T, Awais M and Sajid M 2011 *Int. J. Mod. Phys. B* **25** 2863
[11] Fung Y C 1984 *Biodynamics Circulation* (New York: Springer-Verlag)
[12] Dash R K, Mehta K N and Jayaraman G 1996 *Int. J. Eng. Sci.* **34** 1145
[13] Eldabe N T M and Salwa M G E 1995 *J. Phys. Soc. Jpn.* **64** 41
[14] Boyd J, Buick J M and Green S 2007 *Phys. Fluids* **19** 93
[15] Nadeem S, Haq Ul R, Sher Akbar N and Khan Z H 2013 *Alexandria Eng. J.* **52** 577
[16] Gupta P S and Gupta A S 1977 *Can. J. Chem. Eng.* **55** 744
[17] Magyari E and Keller B 1999 *J. Phys. D: Appl. Phys.* **32** 577
[18] Elbashbeshy E M A 2001 *Arc. Mech.* **53** 643
[19] Parhta M K, Murthy P V S N and Rajasekhar G P 2005 *Heat Mass Transfer* **41** 360
[20] Khan S K 2006 *Int. J. Appl. Mech. Eng.* **11** 321
[21] Sanjayanand E and Khan S K 2006 *Int. J. Thermal Sci.* **45** 819
[22] Al-Odat M Q, Damesh R A and Al-Azab T A 2006 *Int. J. Appl. Mech. Eng.* **11** 289
[23] Sajid M and Hayat T 2008 *Int. Commn. Heat Mass Transfer* **35** 347
[24] Bidin B and Nazar R 2009 *Euro. J. Sci. Res.* **33** 710
[25] Bararnia H, Gorji M, Domairry G and Ghotbi A R 2009 *Acta Appl. Math.* **106** 125
[26] El-Aziz M A V 2009 *Can. J. Phys.* **87** 359
[27] Pal D 2010 *Appl. Math. Comput.* **217** 2356
[28] Nadeem S, Zaheer S and Fang T 2011 *Numer. Algor.*
[29] Ishak A 2011 *Sains Malaysiana* **40** 391
[30] Sahoo B and Poncet S 2011 *Int. J. Heat Mass Transfer* **54** 5010
[31] Mukhopadhyay S and Gorla R S R 2012 *Heat Mass Transfer* (in press)
[32] Nadeem S, Haq Ul R and Lee C 2012 *Scientia Iranica* **19** 1550
[33] Elbashbeshy E M A 1998 *J. Phys. D: Appl. Phys.* **31** 1951
[34] Elbashbeshy E M A and Bazid M A 2002 *Appl. Math. Comput.* **125** 317
[35] Ishak A, Nazar R and Pop I 2008 *Phys. Lett. A* **372** 559
[36] Rahman M M and Sultana T 2008 *Nonlinear Anal.: Model. Control* **13** 71
[37] Liu I C 2005 *Int. Comm. Heat Mass Transfer* **32** 1075
[38] Ishak A, Nazar R and Pop I 2009 *Heat Mass Transfer* **45** 563
[39] Aman F and Ishak A 2010 *Heat Mass Transfer* **46** 615
[40] Bhattacharyya K 2013 *Chin. Phys. B* **22** 074705
[41] Brewster M Q 1972 *Thermal Radiative Transfer Properties* (New York: Wiley)
[42] Bhattacharyya K 2011 *Chin. Phys. Lett.* **28** 074701